



# Phase trapping and slipping in a forced hydrodynamically self-excited jet

Larry K. B. Li<sup>†</sup> and Matthew P. Juniper

Department of Engineering, University of Cambridge, Trumpington Street, Cambridge CB2 1PZ, UK

(Received 29 July 2013; revised 9 September 2013; accepted 3 October 2013)

In a recent study on a coupled laser system, Thévenin *et al.* (*Phys. Rev. Lett.*, vol. 107, 2011, 104101) reported the first experimental evidence of phase trapping, a partially synchronous state characterized by frequency locking without phase locking. To determine whether this state can arise in a hydrodynamic system, we reanalyse the data from our recent experiment on a periodically forced self-excited low-density jet (*J. Fluid Mech.*, vol. 726, 2013, pp. 624–655). We find that this jet exhibits the full range of phase dynamics predicted by model oscillators with weak nonlinearity. These dynamics include (i) phase trapping between phase drifting and phase locking when the jet is forced far from its natural frequency and (ii) phase slipping during phase drifting when it is forced close to its natural frequency. This raises the possibility that similar phase dynamics can be found in other similarly self-excited flows. It also strengthens the validity of using low-dimensional nonlinear dynamical systems based on a universal amplitude equation to model such flows, many of which are of industrial importance.

**Key words:** absolute/convective instability, flow control, nonlinear dynamical systems

## 1. Introduction

When a self-excited oscillator is periodically forced at a frequency different from its natural frequency, it can respond by adjusting its oscillation frequency towards that of the forcing. This adjustment process is known as synchronization and was first discovered by Huygens (1673) in coupled pendulum clocks. Since then, it has been identified in a variety of natural systems (e.g. flashing fireflies, circadian rhythms, and clapping spectators) and has been used in the operation of artificial systems (e.g. triode circuits, electromagnetic lasers, and cardiac pacemakers).

Weakly nonlinear analysis of model oscillators shows that several different stable states are possible. Some of these states, such as *phase drifting* and *phase locking*, have been observed in experiments on a variety of systems. One particular state, however, known as *phase trapping*, has only recently been observed in an experiment,

<sup>†</sup> Email address for correspondence: [l.li@gatescambridge.org](mailto:l.li@gatescambridge.org)

which was on a coupled laser system (Thévenin *et al.* 2011). In this paper, we report phase trapping for a forced self-excited hydrodynamic system, a forced low-density jet. Before presenting our experimental setup (§ 2) and results (§ 3), we will review the features of model oscillators (§ 1.1) and discuss their relevance to hydrodynamic oscillators (§ 1.2).

### 1.1. Synchronization in model oscillators

For forced synchronization, one of the simplest phenomenological models is the forced van der Pol (1927) (VDP) oscillator:

$$\ddot{z} - \epsilon(1 - z^2)\dot{z} + \omega_0^2 z = B \sin(\omega_f t), \quad (1.1)$$

where the feedback parameter,  $\epsilon$ , controls the degree of both linear self-excitation (power supply) and nonlinear self-limitation (power dissipation). The undamped ( $\epsilon = 0$ ) natural frequency is set by  $\omega_0$ , and the damped ( $\epsilon > 0$ ) natural frequency is denoted by  $\omega_n$ .

In the limit of weak nonlinearity ( $0 < \epsilon \ll 1$ ), the approximate solutions to (1.1) can be found analytically through the Krylov–Bogoliubov method of averaging. For this paper, we focus only on the key results, which are valid for the entire class of low-dimensional dynamical models derived from the universal amplitude equation (i.e. the normal form) for a periodically forced self-excited system near its supercritical Hopf point (for details, see § 7.2 of Pikovsky *et al.* 2003). In figure 1, we sketch the synchronization diagram for such a model oscillator. There are four main states:  $\mathbb{A}$ ,  $\mathbb{B}$ ,  $\mathbb{C}$ , and  $\mathbb{D}$ . The dynamical transitions between them are described in the figure caption, and their individual characteristics are listed in table 1.

All four states arise from synchronization, but only two ( $\mathbb{C}$ ,  $\mathbb{D}$ ) are fully synchronous in that both their phase and frequency are locked into the forcing. This means that they exhibit both (i) *phase locking*, a condition for which the difference between the instantaneous phase of the forced oscillator and that of its forcing,  $\Psi(t) \equiv \psi_u(t) - \psi_f(t)$ , is constant in time; and (ii) *frequency locking*, a condition for which the time-averaged frequency of the forced oscillator is equal to that of its forcing:  $\langle \dot{\Psi}(t) \rangle = 0$ . In keeping with the literature, we refer to states  $\mathbb{C}$  and  $\mathbb{D}$  as *phase locking*, even though they involve both phase locking and frequency locking. For regular systems, this terminology is acceptable because phase locking requires frequency locking, although frequency locking does not require phase locking. Situated between one of the fully synchronous states ( $\mathbb{D}$ ) and the asynchronous state ( $\mathbb{A}$ ) is a partially synchronous state ( $\mathbb{B}$ ) in which frequency locking occurs without phase locking. In other words,  $\langle \dot{\Psi}(t) \rangle = 0$  and  $\Psi(t)$  neither remains constant nor increases or decreases unboundedly. Instead  $\Psi(t)$  oscillates boundedly around a fixed value as though it is trapped, which is why this state ( $\mathbb{B}$ ) is often called *phase trapping* (Aronson, Ermentrout & Kopell 1990).

### 1.2. Synchronization in hydrodynamic oscillators

According to Pikovsky *et al.* (2003), the four synchronization states that arise in model oscillators (§ 1.1) should be universal to all periodically forced self-excited systems with a single weakly nonlinear oscillatory mode. To date, however, only partial evidence of such universality has been demonstrated in hydrodynamic systems. Phase locking ( $\mathbb{C}$ ,  $\mathbb{D}$ ) and phase drifting ( $\mathbb{A}$ ) have both been observed in a variety of open self-excited flows: cylinder wakes (Provansal, Mathis & Boyer 1987; Karniadakis & Triantafyllou 1989), capillary jets (Olinger 1992), low-density jets (Sreenivasan, Raghun & Kyle 1989; Hallberg & Strykowski 2008), low-density and equidensity

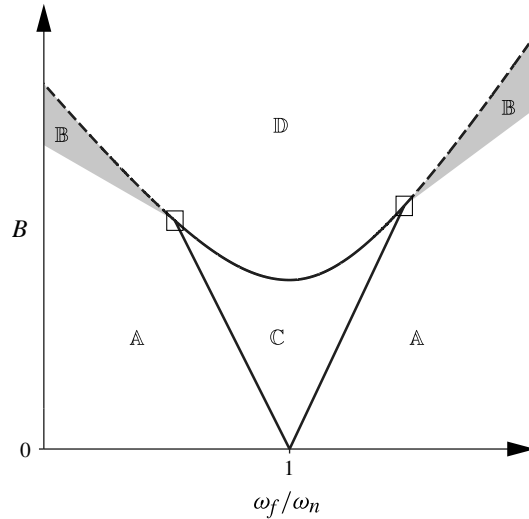


FIGURE 1. Synchronization diagram for a periodically forced self-excited model oscillator with weak nonlinearity, such as the forced VDP oscillator with small  $\epsilon$  (1.1). This diagram is adapted from figure 7.6 of Pikovsky, Rosenblum & Kurths (2003) and figures 3.5–3.9 of Balanov *et al.* (2009). It is centred on the 1:1 Arnol’d tongue, and its parameter space is defined by the normalized forcing frequency ( $\omega_f/\omega_n$ ) and the forcing amplitude ( $B$ ). The characteristics of the four synchronization states (A, B, C, D) are listed in table 1. Regions of phase trapping (B) are shown in grey shading. The solid lines denote saddle-node (blue-sky) bifurcations, and the dashed lines denote torus-death (inverse Neimark–Sacker) bifurcations. The horizontal axis ( $B = 0$ ) coincides with torus-birth (Neimark–Sacker) bifurcations. In the two boxed regions, complex bifurcations occur, which are not illustrated here but are discussed by Holmes & Rand (1978).

State	Name	$\Psi(t)$	$Z_u(t)$	Global attractor	Macro. dynamics
A	Phase drifting	Increases or decreases	Modulated	Torus	Quasiperiodic
B	Phase trapping <sup>a</sup>	Oscillates boundedly	Modulated	Torus	Quasiperiodic
C	Phase locking <sup>b</sup>	Constant	Constant	Limit cycle <sup>c</sup>	Periodic
D	Phase locking <sup>b</sup>	Constant	Constant	Limit cycle	Periodic

TABLE 1. Characteristics of the four synchronization states shown in figure 1 in terms of (i) the difference in instantaneous phase between the forced oscillator and its forcing,  $\Psi(t) \equiv \psi_u(t) - \psi_f(t)$ ; (ii) the instantaneous amplitude of the forced oscillator,  $Z_u(t)$ ; (iii) the global attractor in state space; and (iv) the macroscopic dynamics. States B, C, and D are all frequency-locked, i.e.  $\langle \dot{\Psi}(t) \rangle = 0$ , but only states C and D are also phase-locked, i.e.  $\Psi(t) = \text{constant}$ . <sup>a</sup> This is also known as *imperfect phase locking* (Penelet & Biwa 2013). <sup>b</sup> This is also known as *perfect synchronization* (Penelet & Biwa 2013) or simply *lock-in*. <sup>c</sup> This limit cycle differs from the one for state D in that it exists on the surface of a resonant torus (see figure 3.11 of Balanov *et al.* 2009).

cross-flowing jets (Davitian *et al.* 2010; Getsinger, Hendrickson & Karagozian 2012), and jet diffusion flames (Li & Juniper 2013b). Phase trapping (B), by contrast, has never been observed in any type of flow. Experimental evidence for this intermediate

state has only been reported twice before: first by Thévenin *et al.* (2011) for a coupled laser system and then by Penelet & Biwa (2013) for a forced thermoacoustic system. According to Thévenin *et al.* (2011), this may be because differentiating between phase trapping and standard frequency locking requires delicate control of the experimental conditions.

In this paper, we report on the phase dynamics of a forced self-excited hydrodynamic system, a forced low-density jet. We consider this particular system because we recently showed that its dynamical transitions and bifurcations can be accurately reproduced with a forced VDP oscillator (Li & Juniper 2013a, referred to as LJ 2013). In that study, however, we did not investigate the phase dynamics and therefore could not differentiate between phase drifting (A) and phase trapping (B) – although, through the Poincaré map, we could detect phase locking (C, D). By reanalysing our data with the Hilbert transform, we find phase trapping in a region of parameter space that is consistent with analytical predictions from model oscillators (§ 1.1). We also find phase slipping, a subtle feature of phase drifting that is similarly predicted by model oscillators and is characterized by a nonlinear evolution of  $\Psi(t)$ .

## 2. Experimental setup

Our experimental setup consists of an inertial helium jet discharging into quiescent ambient air from an axisymmetric convergent nozzle. This system is identical to that of our recent study (LJ 2013, § 2.1). Its key feature is that it is purely hydrodynamically self-excited, with an axisymmetric global instability in its potential core (LJ 2013, figure 5), oscillating at a discrete natural frequency of  $f_n = 983.0 \text{ Hz} \pm 0.15\%$  at 95% confidence on the  $t$ -distribution. The primary flow parameters are the density ratio between the jet and its surroundings,  $S \equiv \rho_j/\rho_\infty = 0.14$ ; the transverse curvature,  $d/\theta = 35.5$ , which is the ratio of the nozzle exit diameter to the initial momentum thickness; and the Reynolds number,  $Re \equiv \rho_j U_j d/\mu_j = 1110$ , where  $U_j$  is the time-averaged bulk velocity and  $\mu_j$  is the dynamic viscosity of the jet fluid (helium gas at 293 K and 1 atm). The secondary flow parameters are the Richardson and Mach numbers, but these are both low ( $Ri \equiv gd(\rho_\infty - \rho_j)/\rho_j U_j^2 = 7.4 \times 10^{-4}$  and  $M \equiv U_j/c_\infty = 6.5 \times 10^{-2}$ ), so buoyancy and compressibility effects are negligible.

To induce synchronization, we force the jet sinusoidally in time with a loudspeaker mounted upstream. We do this over a range of frequencies ( $0.84 \lesssim f_f/f_n \lesssim 1.16$ ) so as to explore all four states predicted by model oscillators (§ 1.1). These frequencies ( $823 \leq f_f \leq 1143 \text{ Hz}$ ) are sufficiently far from the Helmholtz resonance frequency of the nozzle plenum (380 Hz with helium) that the spectral response of the forcing system, as measured by a condenser microphone at  $(x/d, r/d) = (1.5, 2.0) \pm 0.017$ , is relatively flat. At each forcing frequency,  $f_f$ , we incrementally increase the forcing amplitude,  $A$ , until just beyond the onset of phase locking. We define  $A$  as the peak-to-peak voltage into the loudspeaker, so that it is directly proportional to the acoustic pressure amplitude,  $A = (2904.22 \text{ mV}_{\text{pp}} \text{ Pa}^{-1})|p'_f|$ , where the constant of proportionality is valid to within  $\pm 5.8\%$  over the  $f_f$  range of this study. (This equation is also valid for LJ 2013, although it was not shown there.)

To measure the jet response, we use a hot-wire anemometer positioned in the wavemaker region – on the jet centreline,  $1.5d$  downstream of the nozzle exit:  $(x/d, r/d) = (1.5, 0) \pm 0.017$ . Before a test run, we calibrate the hot wire in helium to a nominal uncertainty of  $\pm 1.7\%$  at 95% confidence on the normal distribution. At each forcing condition, we digitize the output voltage at 16384 Hz for 16 s on a 16 bit data converter, producing a time series of the local streamwise velocity fluctuation,  $u'(t)$ .

We then post-process the data by computing the complex analytic signal via the Hilbert transform:

$$\zeta_u(t) = u'(t) + iu'_H(t) = Z_u(t)e^{i\psi_u(t)}, \quad (2.1)$$

where  $u'_H(t)$  is the Hilbert transform of the jet signal  $u'(t)$ , and  $Z_u(t)$  and  $\psi_u(t)$  are its instantaneous amplitude and instantaneous phase, respectively. By applying the same transform to the forcing signal, we obtain its instantaneous phase,  $\psi_f(t)$ , which we subtract from  $\psi_u(t)$  to get the phase difference:  $\Psi(t) \equiv \psi_u(t) - \psi_f(t)$ . We use  $\Psi(t)$  and  $Z_u(t)$  as our primary indicators of the phase dynamics and amplitude dynamics, respectively. We use the time rate of change of  $\psi_u(t)$ , or  $\dot{\psi}_u(t)$ , as our indicator of the instantaneous jet frequency, making it an amplitude-weighted average of the different frequencies (i.e.  $f_n^*$ ,  $f_f$ , and their linear combinations) that coexist in the signal.

### 3. Results and discussion

Figure 2 shows our experimental data from the jet: figure 2(a) shows its synchronization diagram centred on the 1:1 Arnol'd tongue, with regions of phase trapping in grey shading, and figures 2(b)–2(e) show time traces of  $\Psi(t)$  and  $u'(t)$  for two different forcing frequencies, one close to the natural frequency and one far from it. For ease of comparison, we let  $\Psi(t)$  take any value on the whole real number line (i.e. we do not confine it to the range  $[0, 2\pi]$ ) and reset  $\Psi(t=0)$  to zero in every case. This helps because, to identify the four synchronization states predicted by model oscillators (§ 1.1), we need to consider only the temporal evolution of  $\Psi(t)$  and not its absolute value. In figure 2(c,e) the oscillation envelope of  $u'(t)$  is  $Z_u(t)$ .

#### 3.1. Jet response when $f_f$ is close to $f_n$

We consider the two forcing frequencies in turn, starting with the one close to the natural frequency (figure 2d,e):  $f_f/f_n = 1023 \text{ Hz}/983 \text{ Hz} \approx 1.04$ .

When forced at low amplitudes ( $300 \leq A \leq 500 \text{ mV}_{pp}$ ), the jet responds by phase drifting (A):  $\Psi(t)$  decreases unboundedly with time and  $Z_u(t)$  becomes modulated at the beat frequency,  $|f_f - f_n^*|$ , where the asterisk on  $f_n$  denotes its value as modified by the forcing. This concurs with our recent study (LJ 2013), which showed that the trajectory in state space is on the surface of a stable ergodic  $\mathbb{T}^2$  quasiperiodic attractor created by a torus-birth bifurcation. Here  $\Psi(t)$  decreases because the jet is forced above its natural frequency (if  $f_f/f_n < 1$ ,  $\Psi(t)$  increases). This decrease is not linear in time: there are long periods in which  $\Psi(t)$  is nearly constant, interrupted by short periods in which  $\Psi(t)$  changes rapidly by  $2\pi$ . These short periods coincide with jumps in  $Z_u(t)$  and also occur at the beat frequency. This intermittent behaviour, known as *phase slipping* (Pikovsky *et al.* 2003), is thought to be a universal feature of forced or coupled self-excited systems but, in hydrodynamics, has only previously been observed in the coupling between an elastically mounted rigid cylinder and its self-excited wake (Khalak & Williamson 1999, figure 14). Physically, the occurrence of phase slipping implies that the jet oscillates at almost the same frequency as the forcing signal for a period of time, but then slows down and loses a full cycle over a shorter period of time (if  $f_f/f_n < 1$ , it gains a full cycle). This process repeats to the limit of our finite sampling duration, which contains  $\sim 1.6 \times 10^4$  natural cycles of  $u'(t)$ . It is an intrinsic feature of the system, not an artefact of extrinsic noise. We conclude this because the phase slips always occur unidirectionally and periodically, not randomly in direction or time.

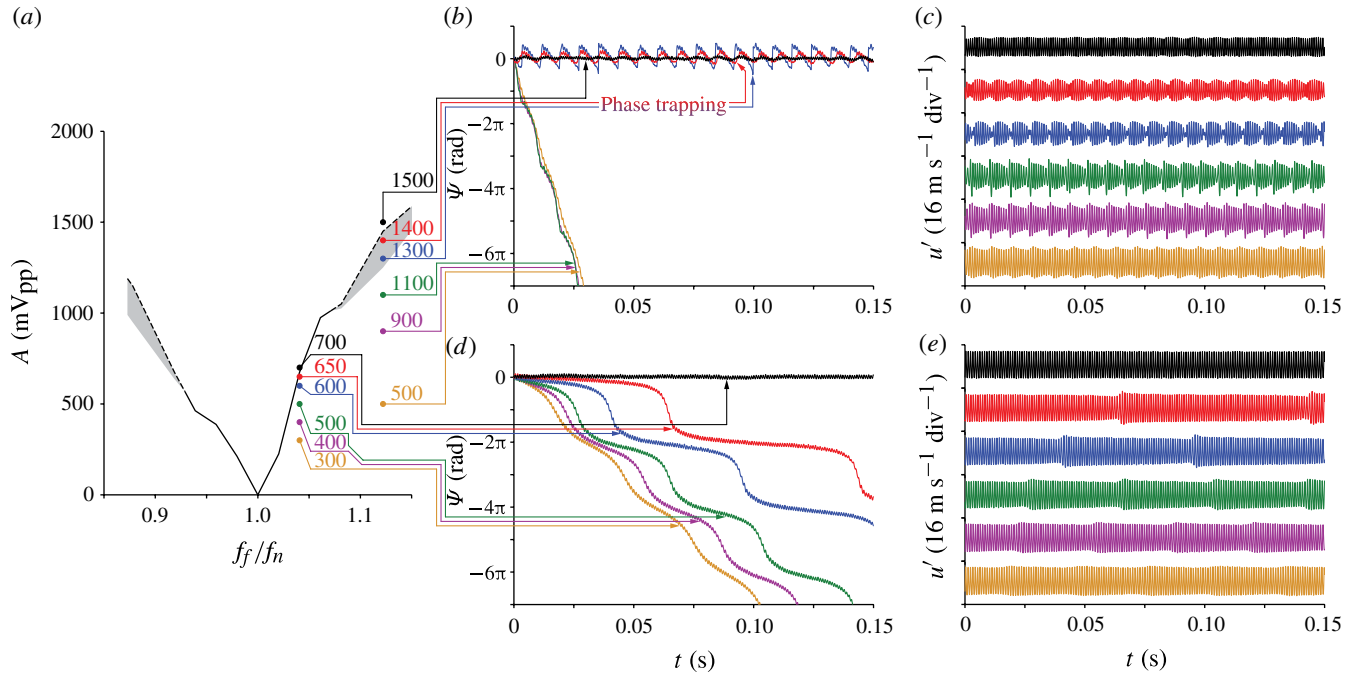


FIGURE 2. Experimental data from the forced low-density jet: (a) its synchronization diagram centred on the 1:1 Arnol'd tongue, with regions of phase trapping in grey shading; and (b–e) time traces of  $\Psi(t)$  and  $u'(t)$  for two different forcing frequencies, one close to the natural frequency (d,e:  $f_f/f_n \approx 1.04$ ) and one far from it (b,c:  $f_f/f_n \approx 1.12$ ). In (a) the solid lines denote saddle-node bifurcations, the dashed lines denote torus-death bifurcations, and the horizontal axis ( $A = 0$ ) coincides with torus-birth bifurcations. In (b,d)  $\Psi(t = 0)$  is reset to zero in every case, which helps when comparing its temporal evolution but means that its absolute value is arbitrary. In (c,e) the oscillation envelope of  $u'(t)$  is  $Z_u(t)$ .

### *Phase trapping and slipping in a forced self-excited jet*

When forced at moderate amplitudes ( $600 \leq A \leq 650 \text{ mV}_{\text{pp}}$ ), the jet continues to respond by phase drifting ( $\mathbb{A}$ ) but with two differences. First, the time-averaged slope of  $\Psi(t)$ , or  $\langle \dot{\Psi}(t) \rangle$ , is pulled towards zero, indicating that the time-averaged frequency of the jet is pulled towards that of the forcing:  $\langle \dot{\psi}_u(t) \rangle \rightarrow \langle \dot{\psi}_f(t) \rangle$ . This process is known as *frequency pulling* (Gyergyek 1999) and can also be detected in the power spectral density (LJ 2013, figures 6*b* and 8*a*:  $f_n^* \rightarrow f_f$  as  $A$  increases). Second, the time interval between successive phase slips increases while the time duration of each phase slip decreases. This occurs because the beat frequency,  $|f_f - f_n^*|$ , which can be approximated by  $|\langle \dot{\Psi}(t) \rangle|/2\pi$ , decreases as  $f_n^*$  is pulled towards  $f_f$ . For  $Z_u(t)$ , this implies increases both in the time interval between successive amplitude jumps and in the suddenness of each amplitude jump. Together, these observations show that, as  $A$  increases, the jet spends progressively more time ( $\propto |f_f - f_n^*|^{-1} \therefore \propto |\langle \dot{\Psi}(t) \rangle|^{-1}$ ) oscillating at  $f_f$  and correspondingly less time phase slipping.

When forced above a critical amplitude ( $A \geq A_{\text{loc}} = 700 \text{ mV}_{\text{pp}}$ ), the jet responds by phase locking ( $\mathbb{C}$ ): both  $\Psi(t)$  and  $Z_u(t)$  become constant with time, indicating that the jet spends all of its time oscillating at  $f_f$ . This concurs with our recent study (LJ 2013), which showed that the trajectory in state space is an isolated closed orbit around a periodic attractor created by a saddle-node bifurcation ( $\mathbb{A} \rightarrow \mathbb{C}$ ). There are, however, very weak oscillations in  $\Psi(t)$  occurring on the same (fast) time scale as  $u'(t)$ . These are present even before the onset of phase locking and arise because the jet does not oscillate perfectly harmonically, whereas the forcing nearly does. Although not shown, our measurements of the near-field pressure spectrum produced by the forcing (without a jet flow) indicate negligible harmonic distortion: over 99.6% of the total disturbance power is contained within a narrow band around the fundamental,  $f_f \pm 0.025\%$ .

#### *3.2. Jet response when $f_f$ is far from $f_n$*

Next we consider the forcing frequency that is far from the natural frequency (figure 2*b,c*):  $f_f/f_n = 1103 \text{ Hz}/983 \text{ Hz} \approx 1.12$ .

When forced at low amplitudes ( $500 \leq A \leq 1100 \text{ mV}_{\text{pp}}$ ), the jet responds by phase drifting ( $\mathbb{A}$ ). This is similar to its behaviour when it is forced close to  $f_n$  (§ 3.1) but with two differences. First,  $\langle \dot{\Psi}(t) \rangle$  is further from zero and does not vary appreciably with  $A$ , which concurs with our observations that there is weaker frequency pulling when  $f_f$  is far from  $f_n$  (LJ 2013, figures 8*a* and 11*b*:  $f_n^*$  remains unchanged from its unforced value  $f_n$  as  $A$  increases). Second, because  $\Psi(t)$  decreases so rapidly, phase slipping is less noticeable, although modulations in  $Z_u(t)$  at the beat frequency ( $|f_f - f_n^*|$  or approximately  $|f_f - f_n| \approx 120 \text{ Hz}$ ) are still detectable.

When forced at moderate amplitudes ( $1300 \leq A \leq 1400 \text{ mV}_{\text{pp}}$ ), the jet responds by phase trapping ( $\mathbb{B}$ ):  $\Psi(t)$  oscillates periodically on the same (beating) time scale as  $Z_u(t)$  but neither increases nor decreases unboundedly. Instead it remains bounded such that  $\langle \dot{\Psi}(t) \rangle$  is exactly zero, indicating frequency locking without phase locking. Physically, the jet maintains this partially synchronous state by periodically switching between two types of oscillation. For a period of time, the jet oscillates more slowly than the forcing signal ( $\dot{\Psi}(t) < 0$ ), losing part of a cycle. Then, over a shorter period of time, the jet speeds up to overtake the forcing ( $\dot{\Psi}(t) > 0$ ), regaining the part of the cycle that it previously lost. This process of slowing down and speeding up (relative to  $f_f$ ) repeats such that the oscillations in  $\Psi(t)$  cancel out over time, leading to frequency locking:  $\langle \dot{\Psi}(t) \rangle = 0$ . The continued modulation of  $Z_u(t)$  is consistent with our observations of a stable (but shrinking) ergodic  $\mathbb{T}^2$  quasiperiodic attractor in state

space (LJ 2013, figure 11c). The presence of phase trapping in this particular region of parameter space is accurately predicted by model oscillators (§ 1.1).

When forced above a critical amplitude ( $A \geq A_{loc} = 1500 \text{ mV}_{pp}$ ), the jet responds by phase locking ( $\mathbb{D}$ ). This is similar to its behaviour when it is forced close to  $f_n$  (§ 3.1) except that this transition ( $\mathbb{B} \rightarrow \mathbb{D}$ ) occurs via a torus-death bifurcation rather than a saddle-node bifurcation ( $\mathbb{A} \rightarrow \mathbb{C}$ ). Both of these bifurcations have been confirmed by nonlinear time-series analysis (LJ 2013) and are accurately predicted by model oscillators (§ 1.1).

### 3.3. *Physical interpretation*

By combining the findings in §§ 3.1 and 3.2 with those of our recent study (LJ 2013), we can form a more complete physical understanding of the way in which synchronization occurs. When the time scales of the forced and natural modes are similar (§ 3.1:  $f_f$  close to  $f_n$ ), synchronization occurs via a gradual pulling of the jet frequency towards the forcing frequency (figure 2d:  $\langle \dot{\Psi}(t) \rangle$  gradually approaches zero as  $A$  increases), resulting in an abrupt decrease in the amplitude of the natural mode at the onset of phase locking (LJ 2013, figure 6b,c: the spectral power at  $f_n^*$  abruptly vanishes when  $A$  reaches  $A_{loc}$  because this is when  $f_n^*$  is pulled exactly to  $f_f$ ). When the time scales of the forced and natural modes are not similar (§ 3.2:  $f_f$  far from  $f_n$ ), synchronization occurs via a gradual decrease in the amplitude of the natural mode without a concurrent pulling of its frequency (LJ 2013, figure 9b), resulting in an abrupt pulling of the jet frequency to the forcing frequency at the onset of phase trapping (figure 2b). Together, these findings show that synchronization can occur via two distinct pathways: (i) it occurs via a change in the phase (frequency) dynamics if the temporal coupling between the forced and natural modes is strong ( $f_f$  close to  $f_n$ ); but (ii) it occurs via a change in the amplitude dynamics if this temporal coupling is weak ( $f_f$  far from  $f_n$ ).

### 3.4. *Low-dimensional modelling*

Having examined the forced low-density jet, we now compare it to a forced low-dimensional model so as to illustrate their similarities with a specific example. For this, we use the forced VDP oscillator (1.1) because it is one of the simplest such models with self-excited temporal solutions, a basic requirement for capturing the self-excited temporal dynamics of the jet. We solve the model numerically using a multistep variable-order algorithm (Shampine & Reichelt 1997). We do this for a feedback parameter of  $\epsilon = 0.2$  because this value is sufficiently small for nonlinearity to be weak, and it places the boundary between saddle-node and torus-death bifurcations (to phase locking) at a forcing frequency that matches that found for the jet (figure 2a):  $|1 - f_f/f_n| \approx 0.07$ . We leave  $\omega_0$  at 1 but explore a range of  $\omega_f$  and  $B$  in order to replicate the experimental conditions. We then post-process the data in the same way as we do the jet data, i.e. by using the Hilbert transform (2.1) to compute the instantaneous amplitude and instantaneous phase.

We show our forced VDP simulations in figure 3, which is analogous to figure 2 (forced jet experiments). Comparing these, we find that nearly all of the jet's phase dynamics, including phase trapping and phase slipping, are accurately reproduced by the forced VDP oscillator. The only feature not reproduced is the fast weak oscillations in  $\Psi(t)$ , which is because the VDP oscillator with  $\epsilon = 0.2$  oscillates more harmonically than does the jet at this operating condition. Apart from this minor discrepancy, the agreement in the phase dynamics is good. This shows that this forced hydrodynamic jet system with infinite degrees of freedom can be modelled reasonably



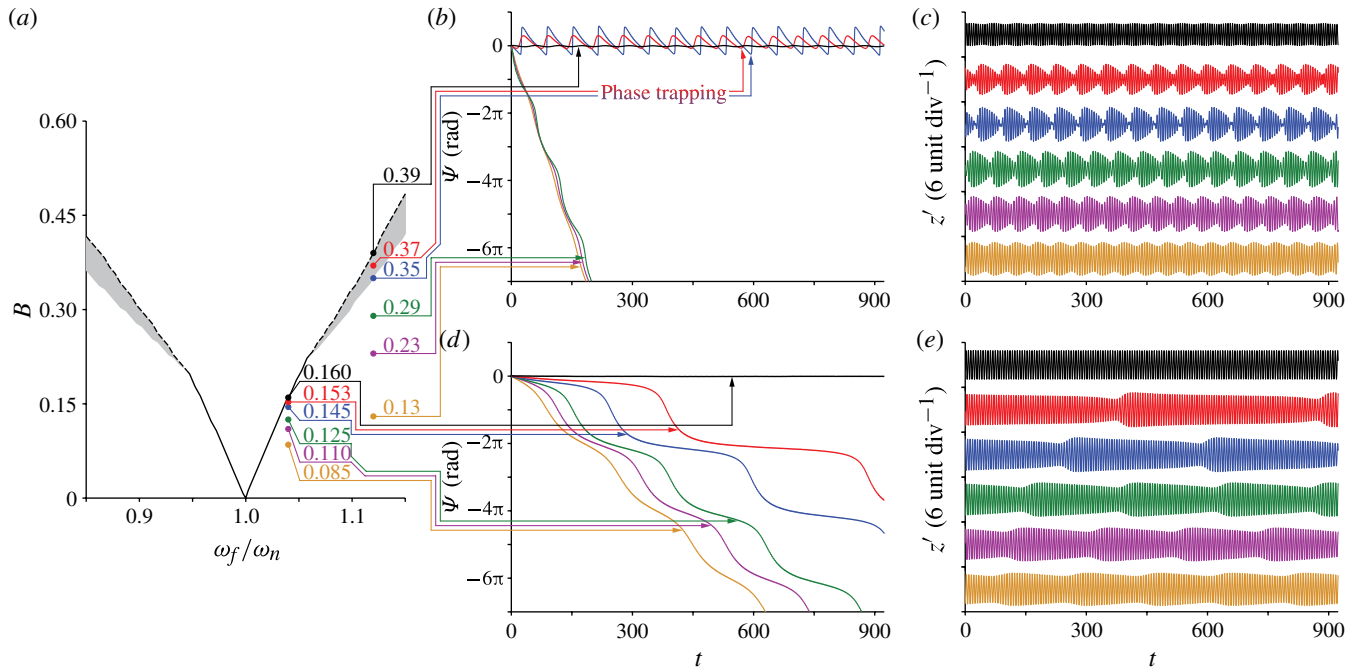


FIGURE 3. The same as for figure 2 but with numerical data from the forced VDP oscillator at  $\epsilon = 0.2$ .

well as a forced nonlinear dynamical system with just three degrees of freedom. This reaffirms the conclusions of our recent study (LJ 2013).

#### 4. Conclusions

We have presented experimental evidence for a range of phase dynamics from a periodically forced self-excited low-density jet, all of which are accurately predicted by model oscillators with weak nonlinearity (§ 1.1). Among the phenomena observed, two are particularly noteworthy. The first is phase trapping, a partially synchronous state that is characterized by frequency locking without phase locking and is found between phase drifting and phase locking when the jet is forced far from its natural frequency (§ 3.2). The second is phase slipping, a subtle feature of phase drifting that is characterized by a nonlinear evolution of the instantaneous phase difference and is found when the jet is forced close to its natural frequency (§ 3.1). To our knowledge, phase trapping has not been observed in a hydrodynamic system before, and phase slipping has only been observed in one experiment on a coupled cylinder-wake system (Khalak & Williamson 1999, figure 14). Both phenomena, however, are potentially important in systems whose stability is determined by mechanisms of energy transfer that depend sensitively on the phase relationship between two or more oscillators of different natural frequencies. For example, these may include vortex-induced vibration in bluff-body wakes and thermoacoustic instability in combustion devices, in which heat-release oscillations caused by a thermoacoustic mechanism can synchronize with those caused by a hydrodynamic mechanism (Chakravarthy *et al.* 2007). A promising way to analyse such problems is to model the overall system as a set of coupled low-dimensional oscillators (e.g. based on a VDP-type kernel), with at least one representing the self-excited hydrodynamics (Monkewitz 1996; Meliga & Chomaz 2011). Hence, in experimentally demonstrating the existence of the full range of phase dynamics in a real self-excited jet, we strengthen the validity of this modelling approach. With further analysis, this should lead to a better understanding of the physical processes operating in the jet, as well as to a more accurate theoretical framework for designing and testing new control strategies. Finally, our results raise the possibility that similar phase dynamics can be found in other similarly self-excited flows, including some industrially relevant sprays (Mehdi-Nejad, Farhadi & Ashgriz 2005) and flames (Emerson *et al.* 2012).

#### Acknowledgements

We would like to thank the Bill & Melinda Gates Foundation, Trinity College Cambridge and the European Research Council (Grant Number 259620) for their financial support. We would also like to thank D. Durox from École Centrale de Paris for loaning us his nozzle.

#### References

- ARONSON, D. G., ERMENTROUT, G. B. & KOPELL, N. 1990 Amplitude response of coupled oscillators. *Physica D* **41** (3), 403–449.
- BALANOV, A., JANSON, N., POSTNOV, D. & SOSNOVTSEVA, O. 2009 1:1 forced synchronization of periodic oscillations. In *Synchronization: From Simple to Complex*, chap. 3. Springer.
- CHAKRAVARTHY, S. R., SHREENIVASAN, O. J., BOEHM, B., DREIZLER, A. & JANICKA, J. 2007 Experimental characterization of onset of acoustic instability in a nonpremixed half-dump combustor. *J. Acoust. Soc. Am.* **122** (1), 120–127.

*Phase trapping and slipping in a forced self-excited jet*

- DAVITIAN, J., GETSINGER, D., HENDRICKSON, C. & KARAGOZIAN, A. R. 2010 Transition to global instability in transverse-jet shear layers. *J. Fluid Mech.* **661**, 294–315.
- EMERSON, B., O'CONNOR, J., JUNIPER, M. & LIEUWEN, T. 2012 Density ratio effects on reacting bluff-body flow field characteristics. *J. Fluid Mech.* **706**, 219–250.
- GETSINGER, D. R., HENDRICKSON, C. & KARAGOZIAN, A. R. 2012 Shear layer instabilities in low-density transverse jets. *Exp. Fluids* **53** (3), 783–801.
- GYERGYEK, T. 1999 Experimental study of the nonlinear dynamics of a harmonically forced double layer. *Plasma Phys. Control. Fusion* **41** (2), 175–190.
- HALLBERG, M. P. & STRYKOWSKI, P. J. 2008 Open-loop control of fully nonlinear self-excited oscillations. *Phys. Fluids* **20** (4), 041703.
- HOLMES, P. J. & RAND, D. A. 1978 Bifurcations of the forced van der Pol oscillator. *Q. Appl. Maths* **35**, 495–509.
- HUYGENS, C. 1673 The pendulum clock. In *Horologium Oscillatorium*. Iowa State University Press, (translated in 1986).
- KARNIADAKIS, G. E. & TRIANTAFYLLOU, G. S. 1989 Frequency selection and asymptotic states in laminar wakes. *J. Fluid Mech.* **199**, 441–469.
- KHALAK, A. & WILLIAMSON, C. H. K. 1999 Motions, forces and mode transitions in vortex-induced vibrations at low mass-damping. *J. Fluid Struct.* **13**, 813–851.
- LI, L. K. B. & JUNIPER, M. P. 2013a Lock-in and quasiperiodicity in a forced hydrodynamically self-excited jet. *J. Fluid Mech.* **726**, 624–655.
- LI, L. K. B. & JUNIPER, M. P. 2013b Lock-in and quasiperiodicity in hydrodynamically self-excited flames: experiments and modelling. *Proc. Combust. Inst.* **34** (1), 947–954.
- MEHDI-NEJAD, V., FARHADI, F. & ASHGRIZ, N. 2005 Naturally induced oscillations in twin-fluid atomizers. In *18th Annual Conference on Liquid Atomization and Spray Systems*. ILASS Americas.
- MELIGA, P. & CHOMAZ, J. M. 2011 An asymptotic expansion for the vortex-induced vibrations of a circular cylinder. *J. Fluid Mech.* **671**, 137–167.
- MONKEWITZ, P. A. 1996 Modelling of self-excited wake oscillations by amplitude equations. *Exp. Therm. Fluid Sci.* **12** (2), 175–183.
- OLINGER, D. J. 1992 Lock-in states in the dripping mode of the capillary jet. *Exp. Fluids* **15** (2), 155–158.
- PENELET, G. & BIWA, T. 2013 Synchronization of a thermoacoustic oscillator by an external sound source. *Am. J. Phys.* **81** (4), 290–297.
- PIKOVSKY, A. S., ROSENBLUM, M. G. & KURTHS, J. 2003 *Synchronization: A Universal Concept in Nonlinear Sciences*. Cambridge University Press.
- VAN DER POL, B. 1927 Forced oscillations in a circuit with nonlinear resistance. *Phil. Mag.* **3** (13), 65–80.
- PROVANSAL, M., MATHIS, C. & BOYER, L. 1987 Bénard–von Kármán instability: transient and forced regimes. *J. Fluid Mech.* **182**, 1–22.
- SHAMPINE, L. F. & REICHEL, M. W. 1997 The MATLAB ODE suite. *SIAM J. Sci. Comput.* **18** (1), 1–22.
- SREENIVASAN, K. R., RAGHU, S. & KYLE, D. 1989 Absolute instability in variable density round jets. *Exp. Fluids* **7** (5), 309–317.
- THÉVENIN, J., ROMANELLI, M., VALLET, M., BRUNEL, M. & ERNEUX, T. 2011 Resonance assisted synchronization of coupled oscillators: frequency locking without phase locking. *Phys. Rev. Lett.* **107** (10), 104101.